ELSEVIER

Nuclear Instruments and Methods in Physics Research A 463 (2001) 634–652

NUCLEAR INSTRUMENTS & METHODS IN PHYSICS RESEARCH Section A

www.elsevier.nl/locate/nima

Transmutation of ^{129}I and ^{237}Np using spallation neutrons produced by 1.5, 3.7 and 7.4 GeV protons

J.-S. Wan[a,1], Th. Schmidt[a], E.-J. Langrock[a,2], P. Vater[a], R. Brandt[a,*], J. Adam[b,3], V. Bradnova[b], V.P. Bamblevski[b], L. Gelovani[b,4], T.D. Gridnev[b], V.G. Kalinnikov[b], M.I. Krivopustov[b], B.A. Kulakov[b], A.N. Sosnin[b], V.P. Perelygin[b], V.S. Pronskikh[b], V.I. Stegailov[b], V.M. Tsoupko-Sitnikov[b], G. Modolo[c], R. Odoj[c], P.-W. Phlippen[c], M. Zamani-Valassiadou[d], J.C. Adloff[e], M. Debeauvais[e], S.R. Hashemi-Nezhad[f], S.-L. Guo[g], L. Li[g], Y.-L. Wang[g], K.K. Dwivedi[h,5], I.V. Zhuk[i], S.F. Boulyga[i], E.M. Lomonossova[i], A.F. Kievitskaja[i], I.L. Rakhno[i], S.E. Chigrinov[i], W.B. Wilson[j]

[a] *Institut für Physikalische Chemie, Kernchemie und Makromolekulare Chemie, FB 15, Marburg, Germany*
[b] *Joint Institute for Nuclear Research, JINR, Dubna, Russian Federation*
[c] *Institut für Sicherheitsforschung, Forschungszentrum Jülich, Jülich, Germany*
[d] *Physics Department, Aristotle-University, Thessaloniki, Greece*
[e] *Institute de Recherche Subatomique, Strasbourg, France*
[f] *Department of High Energy Physics, School of Physics, University of Sydney, Sydney, Australia*
[g] *China Institute of Atomic Energy, Beijing 102413, People's Republic of China*
[h] *Department of Chemistry, North-Eastern Hill University, Shillong, India*
[i] *Institute of Power Engineering Problems, IPEP, Minsk, Belarus*
[j] *Los Alamos National Laboratory, Los Alamos, NM, USA*

Abstract

Small samples of ^{129}I and ^{237}Np, two long-lived radwaste nuclides, were exposed to spallation neutron fluences from relatively small metal targets of lead and uranium, that were surrounded with a 6 cm thick paraffin moderator, and irradiated with 1.5, 3.7 and 7.4 GeV protons. The (n,γ) transmutation rates were determined for these nuclides. Conventional radiochemical La- and U-sensors and a variety of solid-state nuclear track detectors were irradiated simultaneously with secondary neutrons. Compared with results from calculations with well-known cascade codes

*Corresponding author. Fax: +49-6421-285-430.
E-mail address: brandtr@mailer.uni-marburg.de (R. Brandt).

[1] Permanent address: Northwest Institute of Nuclear Technology, Xian, China.
[2] Permanent address: Forschungsbüro Dr. Langrock, Hoyerswerda, Germany.
[3] Permanent address: Nuclear Physics Institute, Rez, Czech Republic.
[4] Permanent address: National Physics Institute of Science, Tiblissi, Georgia.
[5] Present address: Arunachal University, Rono Hills, Itanagar, India.

0168-9002/01/$ - see front matter © 2001 Elsevier Science B.V. All rights reserved.
PII: S0168-9002(01)00175-9

(LAHET from Los Alamos and DCM/CEM from Dubna), the observed secondary neutron fluences are larger. © 2001 Elsevier Science B.V. All rights reserved.

Keywords: Transmutation; ^{129}I-target; ^{237}NP-target; ^{239}Pu production; Spallation neutrons; LAHET code; DCM/CEM code

1. Introduction

During the past decade there has been a revived interest in accelerator driven transmutation technology as an alternative to conventional methods of nuclear energy production and waste disposal, and progress has been made in the design of suitable high-intensity, high-energy proton accelerators as well as of other essential components of a transmutation system. Applications of this technology are therefore being considered that will have industrial as well as social consequences, some aspects of which can be summarized as follows:

1. The economical and safe production of electricity in subcritical nuclear power plants, as suggested for instance by Tolstov [1] and by Rubbia and coworkers [2], becomes feasible. Such facilities would have certain advantages in their construction and operation (no risk of Chernobyl type). However, they are not free of technical risks. When operated with thorium as nuclear fuel, they do avoid the production of problematic transuranium nuclides, in particular of plutonium.
2. The use of the same technology to transmute long-lived radioactive waste nuclei, such as ^{129}I, ^{99}Tc and the minor actinides (Np-, Am-, Cm-isotopes) into stable or short-lived products as originally suggested at Los Alamos National Laboratory (e.g. Ref. [3] and, for an update, the article in this issue about the US nuclear waste transmutation program), could help to solve the problem of nuclear waste storage. One would only need final depositories which must be kept separated from the biosphere for about 600 yr instead of millions of years.
3. Aspects of the new technology need careful monitoring—for example by the IAEA (Vienna)—so that the techniques that would become available are not misused for the production of materials which require strictest surveillance due to international treatises. Recent experimental measurements of the transmutation rates of uranium into plutonium in subcritical systems show that these rates are by no means trivial from a practical point of view [4–7,9]. Subcritical systems that burn uranium rather than thorium will, therefore, require the same careful monitoring that is supposed to be applied to conventional reactors. Thorium burning systems also produce ^{233}U, which is fissionable, but should not be suitable as a weapon material, according to Ref. [2].

Until recently, there has been an abundance of theoretical publications on various aspects of nuclear waste transmutation, while the empirical situation has been studied to a much lesser extent. To our knowledge, there exist only two communications on the experimental transmutation of ^{129}I and ^{237}Np using relativistic particle beams [8,9]. These two nuclides are problem nuclides of radwaste due to their very long half-lives ($> 10^5$ a). In this work we extend the previous studies of the transmutation of ^{129}I and ^{237}Np by using 1.5, 3.7 and 7.4 GeV protons.

As the direct transmutation rates are obviously the result of specific experimental arrangements, we have tried to generalize our results to some extent. For this reason, we studied the number of secondary neutrons produced in our setup, using a variety of radiochemical and solid-state-nuclear-track techniques (SSNTD). These results were compared to theoretical model calculations such as LAHET (Los Alamos) and DCM/CEM (Dubna). Furthermore, a comparison was made with the published experimental results from the Rubbia group at CERN [10]. Finally, we present the results in terms of conventional (n,γ)-cross-sections

for the transmutation of ^{129}I and ^{237}Np under our experimental conditions.

2. Experimental

The experiments were carried out at the Synchrophasotron, Laboratory for High Energies (LHE), Joint Institute for Nuclear Research (JINR), Dubna, Russia. Some details of the irradiation are given in Tables 1 and 2. The different experiments will be described consecutively.

During the 1997 experiment, we had some technical problems determining the proton fluences at 1.5 and 7.4 GeV energy. We employed the radiochemical sensor Al $\rightarrow$ ^{24}Na in close contact to the thick metal target. It is known from the literature [11] and our own recent work [12] that under these conditions, due to ^{27}Al(n,α)^{24}Na reactions, one obtains significantly incorrect results. Consequently, we used in this case the reaction U $\rightarrow$ ^{24}Na as sensor, with the thin uranium foil placed in front of the metallic target [9]. The experimental uncertainty is correspondingly large. We carried out another experiment at 1.5 GeV in 1998 with two independent radiochemical sensors: Al $\rightarrow$ ^{24}Na at 30 cm distance upstream and Cu $\rightarrow$ ^{24}Na in contact and 30 cm upstream from the thick target. The Dubna machine operators determined, within ($\pm$ 10%), the same proton fluences. In addition, we determined the fluence in the (1.5 GeV p + U [Pb]) irradiation with an U $\rightarrow$ ^{24}Na sensor, confirming the values given by the machine operators.

2.1. Transmutation experiments on ^{129}I and ^{237}N

The Pb target (Fig. 1), a cylinder of 20 cm Pb, composed of 20 disks, each 8 cm in diameter and 1 cm thick, was irradiated with a well-focused beam of 1.5, 3.7 and 7.4 GeV protons. The fluence was about 10^{13} protons. The full-width at half-maximum of the beam was about 22 mm as measured with SSNTD in front of the first Pb disk (see Ref. [6] and Section A.7). The Pb cylinder was surrounded by a 6 cm thick paraffin moderator.

This target set-up was chosen because this collaboration has made all its measurements with 20 cm long metallic targets, using a wide variety of projectiles and energies, even though that 20 cm length is considerably shorter than the range of GeV protons. In the same way we chose 6 cm paraffin as moderator. The induced activities could thus be measured radiochemically under the same experimental conditions [5–9,19].

Transmutation studies were also carried out using a similar uranium target (Fig. 2) in order to investigate the influence of the Z of the metallic target and the amount of secondary neutrons

Table 2
Experiment with ^{129}I and ^{237}Np directly exposed to a 3.7 GeV proton beam (1996)

Experiment	Beam-time	Fluence	Radiochemical sensor
3.7 GeV p + ^{129}J/^{237}Np	0.25 h	1.25×10^{13} ($\pm$ 15%)	Cu $\rightarrow$ ^{24}Na

Table 1
Experiments with ^{129}I and ^{237}Np using Pb and U (Pb) targets as a neutron spallation source (3.7 GeV p in 1996; 1.5 GeV p and 7.4 GeV p in 1997). The fluences were measured radiochemically, as indicated

Experiment	Beam-time (h)	Fluence	Radiochemical sensor
1.5 GeV p + Pb	1.17	1.40×10^{13} ($\pm$ 20%)	
1.5 GeV p + U (Pb)	2.14	1.50×10^{13} ($\pm$ 20%)	U $\rightarrow$ ^{24}Na
3.7 GeV p + Pb	0.15	1.24×10^{13} ($\pm$ 15%)	Cu $\rightarrow$ ^{24}Na
3.7 GeV p + U (Pb)	0.27	1.24×10^{13} ($\pm$ 15%)	Cu $\rightarrow$ ^{24}Na
7.4 GeV p + Pb	1.36	0.90×10^{13} ($\pm$ 20%)	
7.4 GeV p + U (Pb)	3.35	0.90×10^{13} ($\pm$ 20%)	U $\rightarrow$ ^{24}Na

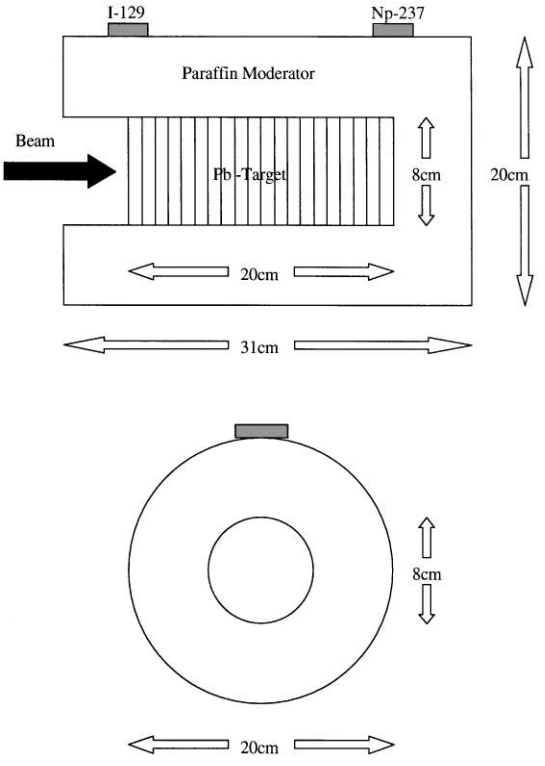

Fig. 1. ^{129}I and ^{237}Np samples on top of the Pb target (1.5, 3.7 and 7.4 GeV protons), side view and top view.

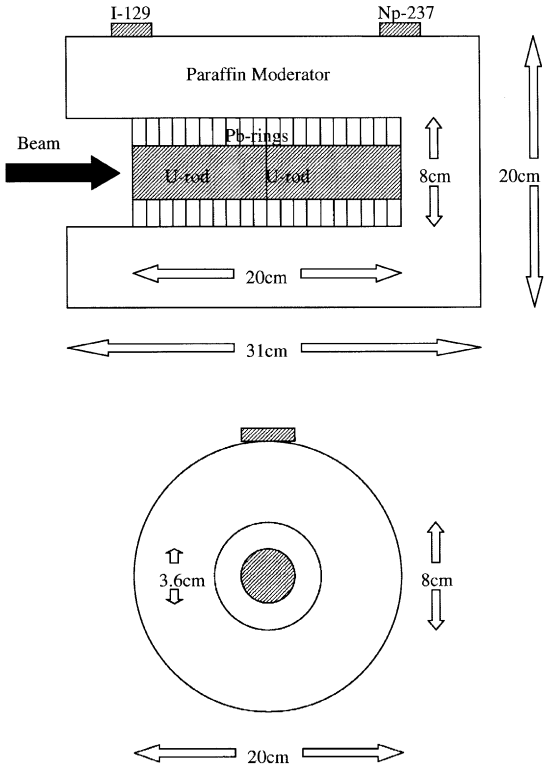

Fig. 2. ^{129}I and ^{237}Np samples on top of the U(Pb) target (1.5 and 7.4 GeV protons), side and top views.

produced. Details of this target, called U (Pb) target, are described in the next section.

On top of the moderator were placed samples of 0.425 g iodine with 15% ^{127}I and 85% ^{129}I (in form of NaI) and of 0.742 g ^{237}Np (in form of NpO_2). The isotopic composition of these iodine samples is typical for the iodine radwaste from a nuclear power plant. It was obtained from the Bochvar Institute in Moscow (VNIINM). The radioactive samples of I and Np were well sealed in Al capsules (Fig. 3). They were prepared by the Institute of Physics and Power Engineering (Obninsk, Russia).

Furthermore, two other ^{129}I and ^{237}Np samples were irradiated directly in the 3.7 GeV proton beam with 1.25×10^{13} protons during a separate irradiation (Fig. 4). After the irradiation, the samples were placed in front of an HPGe-detector to measure the gamma-activity. As both ^{129}I and

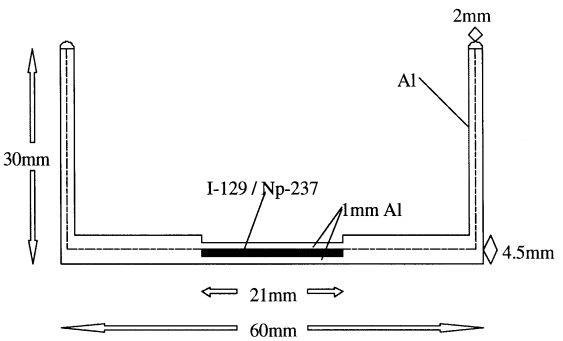

Fig. 3. ^{129}I and ^{237}Np samples in Al container.

^{237}Np samples are fairly radioactive even without any activation, they were placed at a distance of 20 cm from the detector. For the ^{237}Np sample, a Pb plate 1 cm thick was placed between the sample and the detector, reducing considerably the low-energy activity. We identified, using the lead and

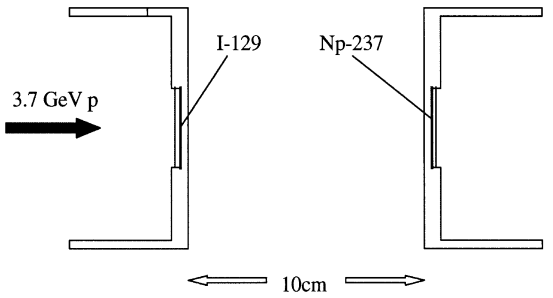

Fig. 4. Setup for the direct irradition of ^{129}I and ^{237}Np with 3.7 GeV protons.

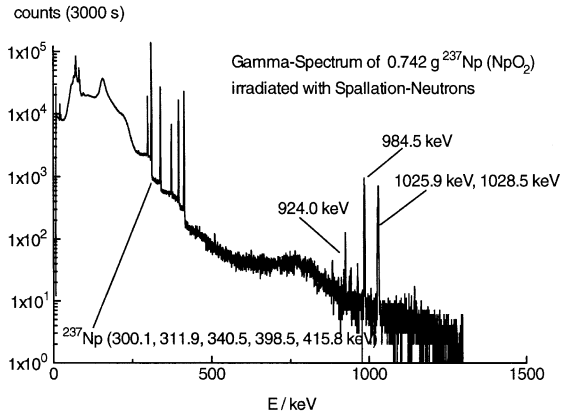

Fig. 5. Spectrum of ^{237}Np irradiated with spallation neutrons from a U target (7.4 GeV p) shielded with 1 cm Pb: ^{238}Np (924, 984, 1026, 1028 keV).

uranium target systems (Figs. 1 and 2), the (n,γ) reaction-products ^{130}I and ^{238}Np (Figs. 5 and 6). The decay curves for these two nuclides have already been published [8,9]. In addition, we could identify also a tiny activity due to ^{126}I in the NaI-samples as shown in the γ-spectra (Fig. 6). Further analysis of the γ-spectra by state-of-the-art techniques is described in Ref. [5–8]. The results are expressed in terms of *breeding rates* $B_{\mathrm{exp}}(\mathrm{A}^Z)$ for the production of the nuclide (A^Z) defined as follows:

$$B_{\mathrm{exp}}(\mathrm{A}^Z) = \frac{\text{number of produced nuclei with } A^z}{(\text{single incident ion})(1\text{ g target isotope})} \quad (1a)$$

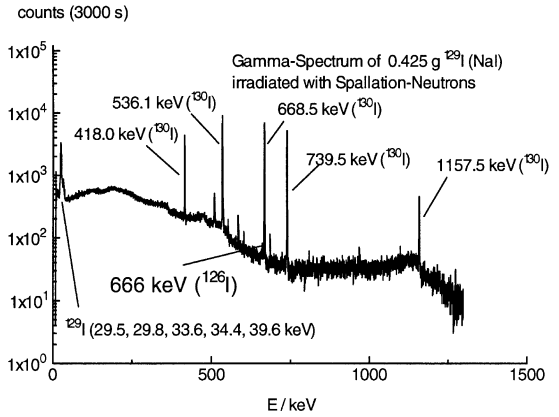

Fig. 6. Spectrum of ^{129}I irradiated with spallation-neutrons from a U-target (7.4 GeV p): ^{130}I (418, 536, 668, 739, 1157 keV).

or formulated in an equivalent manner for proton experiments

$$B_{\mathrm{exp}}(\mathrm{A}^Z) = \frac{\text{total number of produced nuclei with } A^z}{(\text{proton fluence})(1\text{ g target isotope})}. \quad (1b)$$

$B_{\mathrm{exp}}(\mathrm{A}^Z)$ is defined strictly in an empirical manner: It means that ^{129}I is placed at the geometrical position given in Figs. 1 and 2. The resulting B_{exp} values are given in Section 2.2.

In the direct irradiation of ^{129}I and ^{237}Np (Fig. 4) one could observe a large variety of spallation products for ^{129}I as well as some fission products of ^{237}Np as shown in Figs. 7 and 8. Under the experimental conditions available, one could not identify with certainty additional fission products. The experimental results are compared with the results obtained with the semi-empirical formula of Rudstam and others [13–15]. This pattern of observed cross-sections for spallation products of iodine as a function of the mass of the spallation product fits well into the known spallation product behaviour, as described also by Modolo [16].

2.2. Secondary neutron fluence studies with depleted uranium and lanthanum sensors

The ^{129}I and ^{237}Np samples have been irradiated under specific geometric conditions as described

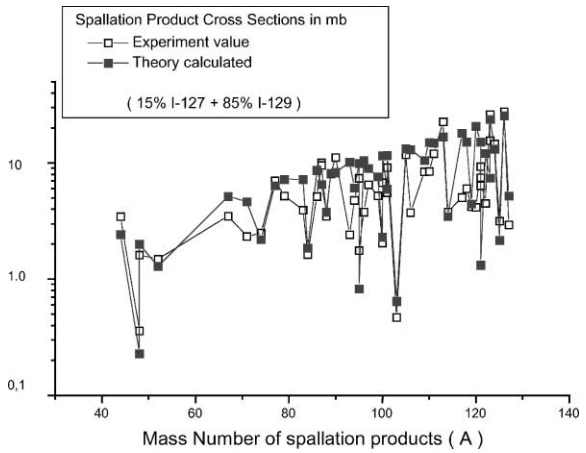

Fig. 7. Cross-section for the spallation products of ^{129}I directly irradiated with 3.7 GeV protons (for details of "Theory calculated", see J.S. Wan, Ph.D.-Thesis, Department of Chemistry, Philipps University, Marburg, Germany, 1999).

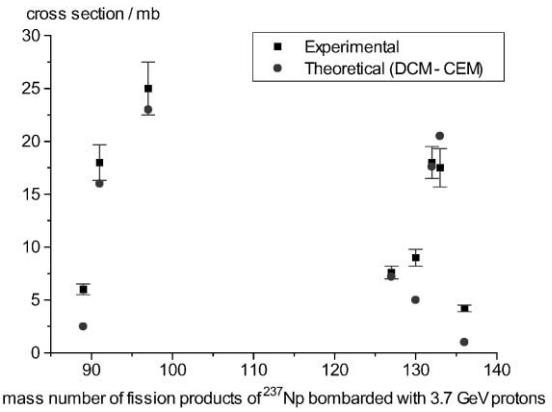

Fig. 8. Cross-section for the fission products of ^{237}Np directly irradiated with 3.7 GeV protons. Theoretical values have been calculated with the DCM/CEM code. For details see text.

above. In order to obtain a more general picture of what is going on physically within the target system, the fluences of secondary neutrons within these target systems themselves were studied. Since it is impossible to measure neutrons with their wide range of energies from thermal up to GeV energies within the relatively small target systems using standard electronic neutron counters, we used a considerably simpler experimental apparatus, i.e. radiochemical and SSNTD-sensors. These techniques give—within limitations—useful results. A preceding paper [9] described in detail how one obtained neutron fluences with a large variety of sensors in the Pb target (Fig. 1) irradiated with 3.7 GeV protons. Here, we present a more generalized method of obtaining neutron fluences in the two targets used for the three proton energies of this study. We describe beforehand the experimental determination of the breeding rates B_{exp}.

The target set-ups for these measurements are shown in Fig. 9. The Pb target (Fig. 1) has already been described as it was used for the ^{129}I and ^{237}Np studies. The uranium target (called U (Pb)-target) is shown in Fig. 2. It contained two rods of natural

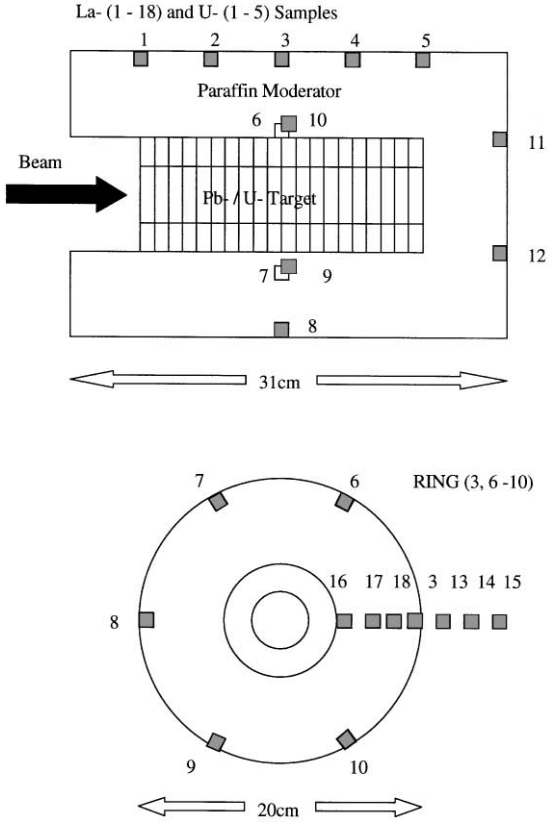

Fig. 9. La and U sensors on the surface of the targets (1.5, 3.7 and 7.4 GeV protons), side view and top view. In positions (1–5), La and U sensors are embeded into the moderator within close proximity of approx. 1 cm from each other.

uranium, 3.6 cm in diameter and 10.5 cm long, encapsuled in thin Al foils and placed in the centre of a lead target 8 cm in diameter and surrounded again by a 6 cm thick paraffin moderator. Both target systems contained small La sensors as well as small U sensors on their surface. In Fig. 9 the La and U sensors are shown.

With the La sensors [1 g La in $(LaCl_3 \cdot (7H_2O))$] one could study the neutron fluence *via* the reaction

$$^{139}\mathrm{La}(n,\gamma)^{140}\mathrm{La} \xrightarrow[T_{1/2}=40\ \mathrm{h}]{\beta^-} {}^{140}\mathrm{Ce} \quad (2)$$

and with the U-sensors [1 g depleted uranium in $(UO_2 \cdot (H_2O))$ with 0.42% ^{235}U] *via* the reaction

$$^{238}\mathrm{U}(n,\gamma)^{239}\mathrm{U} \xrightarrow[T_{1/2}=24\ \mathrm{min}]{\beta^-} {}^{239}\mathrm{Np} \xrightarrow[T_{1/2}=2.3\ \mathrm{d}]{\beta^-} {}^{239}\mathrm{Pu}. \quad (3)$$

After irradiation, the sensors were analysed for their γ activity. The results were registered in the form of B_{exp} values, $B_{exp}(^{140}La)$ and $B_{exp}(^{239}Np)$, on the surface of the moderator. The azimuthally arranged La-sensors, spaced equally (60°) in the middle and on the surface of the moderator, allowed a correction for the azimuthal variation of secondary neutrons due to the non-circular beam distribution of the incident proton flux within a plane perpendicular to the beam direction. With these results one could calculate *average* B_{exp} *values* for ^{140}La and ^{239}Np on the outer mantle of the paraffin moderator for all six target systems studied, as shown in Table 3. The average B_{exp} values of the samples 1–5 on top of the moderator were corrected for the azimutal neutron flux distribution. This procedure is described in earlier publications [6–9]. The B_{exp} values of the ^{129}I and ^{237}Np sensors are shown in Table 4. Obviously, the large experimental uncertainties are entirely due to the uncertainties in the fluence measurements. The activity rates in individual sensors ^{140}La and ^{239}Np could be measured with an uncertainty of $\leqslant 5\%$.

It is interesting to note that all B_{exp} values for ^{140}La and ^{239}Np increase by a factor of (3.5 ± 0.5) with increasing proton energy from 1.5 up to 3.7 GeV. This is slightly more than a linear increase with proton energy. However, we observe only a small increase in B_{exp} values when going from 3.7 up to 7.4 GeV. This is against the experimental evidence from other experiments [17,18] where a slightly less than linear increase with proton energy has been observed. At present we can give no explanation for our results. It cannot be excluded that there have been some

Table 3
Average B_{exp} values for the neutron monitors on the outer surface of the paraffin moderator for Pb and U (Pb) target systems [5–7]

Proton energy (GeV)	Pb target B_{exp} (^{140}La)	Pb target B_{exp} (^{239}Np)	U(Pb) target B_{exp} (^{140}La)	U(Pb) target B_{exp} (^{239}Np)
1.5	$(1.7 \pm 0.4) \times 10^{-4}$	$(0.75 \pm 0.15) \times 10^{-4}$	$(3.1 \pm 0.7) \times 10^{-4}$	$(1.4 \pm 0.3) \times 10^{-4}$
3.7[a]	$(6.0 \pm 0.9) \times 10^{-4}$	$(2.9 \pm 0.4) \times 10^{-4}$	$(10.5 \pm 1.6) \times 10^{-4}$	$(4.5 \pm 0.7) \times 10^{-4}$
7.4	$(7.3 \pm 1.5) \times 10^{-4}$	$(3.3 \pm 0.7) \times 10^{-4}$	$(15.4 \pm 3.1) \times 10^{-4}$	$(6.0 \pm 1.2) \times 10^{-4}$

[a] Taken from Ref. [9].

Table 4
B_{exp} values for the ^{129}I and ^{237}Np samples on the outer surface of the paraffin moderator for Pb and U (Pb) target systems

Proton energy (GeV)	Pb target B_{exp} (^{130}I)	Pb target B_{exp} (^{238}Np)	U(Pb) target B_{exp} (^{130}I)	U(Pb) target B_{exp} (^{238}Np)
1.5	$(0.9 \pm 0.2) \times 10^{-4}$	$(8.1 \pm 1.6) \times 10^{-4}$	$(2.3 \pm 0.5) \times 10^{-4}$	$(9.0 \pm 1.8) \times 10^{-4}$
3.7[a]	$(3.1 \pm 0.5) \times 10^{-4}$	$(44 \pm 7) \times 10^{-4}$	—	—
7.4	$(4.0 \pm 0.8) \times 10^{-4}$	$(41 \pm 9) \times 10^{-4}$	$(14.7 \pm 3.0) \times 10^{-4}$	$(50 \pm 10) \times 10^{-4}$

[a] Taken from Refs. [8,9].

problems with measuring beam intensities at energies above 3 GeV.

It was shown [9] that the experimental $B_{exp}(^{239}Np)$ value for 3.7 GeV proton-induced reactions in the uranium target 10 cm behind the entrance of the beam into U and then 10 cm perpendicular off-axis agreed with the corresponding B_{exp}(fission) value for uranium in the experiment at CERN using 2.7 GeV protons [10]. The experimental results from both laboratories agree, despite some differences in the experimental arrangements. One should remember that is was shown extensively that $B_{exp}(^{239}Np) = (1.10 \pm 0.10) B_{exp}$(fission) in *natural* uranium (0.72% ^{235}U) [9].

This reaction pattern is reproduced when the results of this experiment and of the CERN experiment at a proton energy of 1.5 GeV are compared:

$$B_{exp}(^{239}Np) = (2.2 \pm 0.5)\times 10^{-4} \quad \text{(This work)}$$
$$B_{exp}(\text{fission}) = (3.2 \pm 0.5)\times 10^{-4} \quad \text{(CERN results)}. \qquad [18]$$

Additionally, it is an experimental fact that for a given distance of approx. 10 cm off-axis from the beam direction and 10 cm behind the entrance of the beam into the extended Pb targets, all experimental $B(^{239}Np)$ values for small uranium sensors are in close proximity.

2.3. Estimation of the secondary neutron fluence in our targets and comparison with model calculations

Now one must consider the conversion of B_{exp} values into secondary neutron fluences. The primary relativistic proton (E_P) induces nuclear interactions. This produces a fluence of secondary neutrons with energies $0 < E_N \leqslant E_P$ leaving the outer surface of the moderator. The details of all these nuclear interactions, scattering processes, etc. are certainly quite complex, but the result is simple: One observes experimentally (n,γ) nuclear reaction products, such as ^{140}La and ^{239}Np. High-energy transport codes such as LAHET (Los Alamos) and DCM-CEM (Dubna) that allow the calculation of the secondary neutron fluence $\Phi_n(E)_{theo}$ on the outer surface of the paraffin moderator are based on intra-nuclear cascades using the Bertini model, followed by the pre-equilibrium model and then by the Rutherford–Cameron–Cook–Ignatyuk model giving level densities. These two models have been used by this collaboration for 3.7 GeV protons beforehand [9] and were described in some detail earlier [19]. In this paper we present in Figs. 10 and 11 the calculated $\Phi_n(E)_{theo}$ on the outer mantle of the moderator, as based on these two codes for the reaction (1.5 GeV p + Pb). Furthermore, the excitation function for the (n,γ) reactions (Eqs. (2) and (3)) are well known. Now it is straightforward to calculate a B_{theo} value for all systems investigated:

$$B_{theo}(A^Z) = N_T \int_0^{Ep} \Phi_n(E)\sigma_{(n,\gamma)}(E)\,dE. \qquad (4)$$

$\Phi_n(E)$ is the average energy dependent neutron fluence per cm^2 per proton on the outer surface mantle of the paraffin moderator, the term $\sigma_{(n,\gamma)}(E)$ is the energy dependent (n,γ) neutron capture cross-section, and N_T is the number of target atoms in 1 g of the target-isotope per cm^2. One should remember that the surfaces of our La and U sensors are also about 1 cm^2. The results for all the various B_{theo} are shown in Tables 5 and 6 and compared to the experimental B values, giving a ratio $R(B)$ defined as follows:

$$R(B) = B_{exp}/B_{theo.} \qquad (5)$$

As one can see from Tables 5 and 6, nearly all $R(B)$-values are larger than 1 with a wide spread between (0.7 ± 0.2) and (4.1 ± 0.6). This wide spread in $R(B)$ is not surprising, as both our methods, experimentally and theoretically, are known to be quite approximate. However, we confirm the results from a preceding paper [9] that the discrepancy is larger for such sensors as ^{140}La, which register practically only thermal neutrons, as compared to ^{239}Np, which is also produced to a significant degree by epithermal neutrons. In our experiment one has a very hard neutron spectrum, as shown in Figs. 10 and 11. In Section A.6, it will be shown that no discrepancy can be observed between experiment and theory

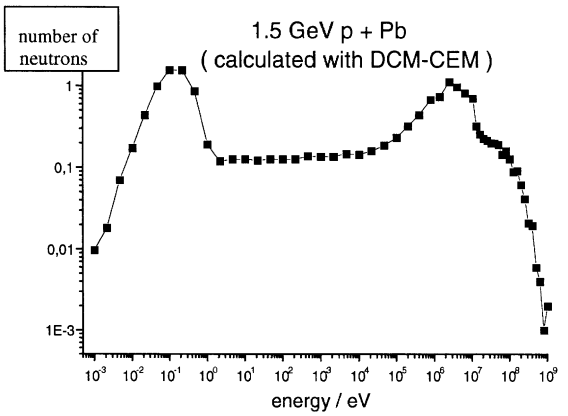

Fig. 10. The neutron spectrum for the reaction (1.5 GeV p + Pb), calculated with the DCM/CEM code on the outer mantle of the moderator for one primary proton. Total number of neutrons:18.6, thermal neutrons ($E < 1$ eV): 5.9. The neutron number on the ordinate is given for the energy bin indicated.

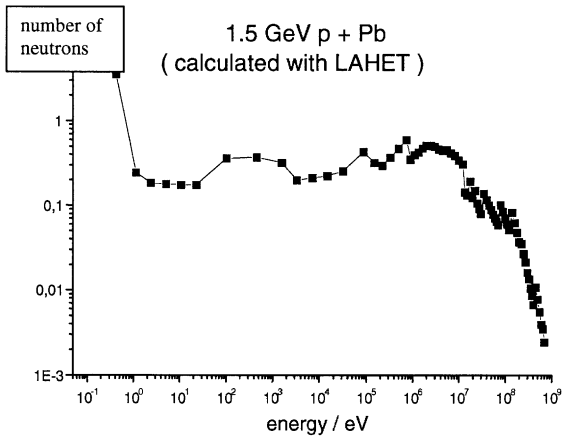

Fig. 11. The neutron spectrum for the reaction (1.5 GeV p + Pb), calculated with the LAHET code on the outer mantle of the moderator for one primary proton. Total number of neutrons: 17.5, thermal neutrons ($E < 1$ eV): 3.8. The neutron number on the ordinate is given for the energy bin indicated.

when only high-energy neutrons ($E > 30$ MeV) are considered.

We encountered rather similar problems [9] when investigating the results of the Rubbia group at CERN [10]: The experimental results for transmutation in uranium agree for the specified geometrical position within both laboratories at 1.5 and (3.2 ± 0.5) GeV proton energy. However, we are unable to understand both experimental results on the basis of model calculations available to us [9].

This discrepancy may be due to one of the following reasons:

1. The theoretical codes underestimate the number of neutrons emitted during the primary interactions of the relativistic proton with the target *or do not take into account correctly the properties of the moderator*. Such an explanation has the difficulty that the LAHET code describes the number of secondary neutrons in close agreement with the experiment when this number is measured with conventional electronic neutron counters within a moderator medium at some (20–40 cm) distance from the beam axis [20].

Table 6
Theoretical B_{theo} values as based on the LAHET-model and comparison with $R(B) = B_{exp}/B_{theo}$

Proton energy (GeV)	$B_{theo}(^{140}La)$ Pb target	$B_{theo}(^{239}Np)$ Pb target
1.5	0.78×10^{-4}	1.02×10^{-4}
	$R(B) = 2.2 \pm 0.5$	$R(B) = 0.7 \pm 0.2$
3.7	1.45×10^{-4}	1.87×10^{-4}
	$R(B) = 4.1 \pm 0.6$	$R(B) = 1.6 \pm 0.3$

Table 5
Theoretical B_{theo} values as based on the DCM-CEM model and the values for $R(B) = B_{exp}/B_{theo}$

Proton energy (GeV)	$B_{theo}(^{140}La)$ Pb target	$B_{theo}(^{239}Np)$ Pb target	$B_{theo}(^{140}La)$ U target	$B_{theo}(^{239}Np)$ U target
1.5	0.82×10^{-4}	0.74×10^{-4}	1.84×10^{-4}	1.65×10^{-4}
	$R(B) = 2.1 \pm 0.5$	$R(B) = 1.0 \pm 0.2$	$R(B) = 1.7 \pm 0.4$	$R(B) = 0.8 \pm 0.2$
3.7	1.50×10^{-4}	1.37×10^{-4}	3.56×10^{-4}	3.28×10^{-4}
	$R(B) = 4.0 \pm 0.8$	$R(B) = 2.1 \pm 0.4$	$R(B) = 2.9 \pm 0.6$	$R(B) = 1.3 \pm 0.3$
7.4	2.38×10^{-4}	1.97×10^{-4}	5.71×10^{-4}	5.34×10^{-4}
	$R(B) = 3.1 \pm 0.6$	$R(B) = 1.7 \pm 0.4$	$R(B) = 2.7 \pm 0.5$	$R(B) = 1.2 \pm 0.3$

2. The theoretical codes give the correct number of secondary neutrons, but these neutrons may show enhanced nuclear cross-sections within about the first 15 cm of interaction [7,9,19].
3. There is an error in the application of the theoretical codes, in which case the preceding paragraph no longer applies.

Our experimental techniques do not allow us at present to decide which option is correct. Consequently, we make an arbitrary choice and consider from now on that the number of secondary neutrons is larger than calculated in order to give some quantitative interpretation to our experimental findings. All excesses of experimental results above theoretical estimations will be considered as being due to larger numbers of secondary neutrons than estimated theoretically. Therefore, we have to estimate the experimental neutron numbers and compare them with theoretical values.

In this estimation of neutron fluences on the outer surface of the paraffin moderator (at $r = 10\,\text{cm}$), the procedure developed by Wan et al. [9] is followed. The total experimental fluence of neutrons $\Phi_n(E)_{exp}$ can be estimated as follows from the experimentally observed B values:

$$\Phi_n(E)_{exp} = \frac{B_{exp} O_s}{N_T \sigma_{eff}(n,\gamma)} \text{(per incident proton)}. \quad (6)$$

The B_{exp} values are given in Tables 3 and 4, O_S is the moderator mantle surface ($2000\,\text{cm}^2$), N_T the number of target atoms in 1 g of the target per cm^2; and $\sigma_{eff}(n,\gamma)$ is the effective (n,γ) cross-section for the neutron energy region in which $\Phi_n(E)_{exp}$ shall be determined. It can be calculated as follows:

$$\sigma_{eff}(n,\gamma) \frac{\int_{E_1}^{E_2} \Phi_n(E)\sigma_{(n,\gamma)}(E)\,dE}{\int_{E_1}^{E_2} \Phi_n(E)\,dE}. \quad (7)$$

The theoretical neutron fluences $\Phi_n(E)_{theor}$ are given in Figs. 10 and 11 (LAHET- and DCM-CEM-code). The neutron energy interval considered—analogous to Ref. [9]—starts with $E_1 = 0\,\text{eV}$ and ends at $E_2 = 1\,\text{eV}$ for the reaction $^{139}\text{La}(n,\gamma)^{140}\text{La}$, since in this neutron energy interval about 90% of the entire B value has been formed [9]. Essentially only low-energy neutrons up to 1 eV contribute substantially to this reaction. In our experiment the corresponding cross-section is $\sigma_{eff}(n,\gamma) = 7.2\,\text{b}$ (see Table 8, Ref. [9]). With this analytical procedure one can calculate the experimental low-energy neutron fluences ($E < 1\,\text{eV}$) for all the reactions studied. Results are given in Table 7 together with the experimental low-energy neutron fluence $\Phi_n(E)_{exp}$ and some theoretical neutron fluences.

Table 7
Some theoretical and experimental neutron fluences on the outer mantle surface of the moderator, normalized to one incident proton

System	n/p[a]	$\Phi_n(E)_{theo}$[b] all energies	$\Phi_n(E)_{theo}$ thermal (<1 eV)	$\Phi_n(E)_{exp}$[c] thermal (<1 eV)
1.5 GeV p + Pb	25.1[d]	18.6[d]	5.9[d]	11 ± 3
		17.5[e]	3.8[e]	
1.5 GeV p + U(Pb)	43[d]	38.2[d]	13[d]	21 ± 5
3.7 GeV p + Pb	43[d]	34.2[d]	10.6[d]	38 ± 6
	41[e]	34.3[e]	7.7[e]	
3.7 GeV p + U(Pb)	79[d]	67.9[d]	25[d]	65 ± 10
7.4 GeV p + Pb	61.5[d]	50.5[d]	17[d]	45 ± 9
7.4 GeV p + U(Pb)	140[d]	117[d]	41[d]	96 ± 20

[a] n/p: Number of secondary neutrons emitted during the nuclear cascade calculation per incident proton.
[b] $\Phi_n(E)_{theo}$: The total neutron fluence on the outer mantle surface calculated by theoretical models.
[c] $\Phi_n(E)_{exp}$: The total experimental low-energy neutron fluence, determined with the La-sensors (for details see text and Eqs. (6) and (7)).
[d] Calculated directly with DCM-CEM code up to 10.4 MeV neutrons.
[e] Calculated directly with LAHET code up to maximum energy neutrons.

The results from Table 7 can be summarized as follows:

(1) Both theoretical models give very similar values for the *total* neutron fluences integrated over all neutron energies, although the amount of low-energy neutrons, as calculated by those two models, differs by up to 50%.
(2) Despite the spread of low-energy neutron fluences calculated theoretically, all experimental low-energy neutron fluences based on La sensors are substantially larger than the theoretical fluences. These results, of course, reflect the results of Tables 5 and 6 with the large values of $R(B)$ in the reaction ^{139}La $(n,\gamma)^{140}$La. Similar calculations can be done for the other neutron sensors, giving rather similar, however, less drastic results.

The results from Table 7 allow an estimation of the low-energy neutron fluence in an accelerator driven subcritical reactor based on our experiments. Although this is a straightforward extrapolation, there appears to be no publication which gives *concrete* neutron fluences for a given *concrete* experimental set-up.

A 10 mA proton beam of 1.5 GeV on a Pb target system (Fig. 1) could produce on the outer surface of the moderator a low-energy neutron fluence in the range of

$$\Phi_{n,exp}(E)_{low\ energy} = (2-4)\times 10^{14} n/s\ cm^{-2}.$$

Technological aspects, such as heat production, radiation damage, etc. are neglected in this estimation. Inside the moderator, the thermal neutron fluences are up to a factor 5 larger than on its surface, as will be shown experimentally in Section A.2 (see also Ref. [9]).

The observed transmutation rates B for ^{129}I and ^{237}Np allow the estimation of the transmutation capacity for a 10 mA/1.5 GeV proton accelerator coupled with a Pb target (Fig. 1) as follows:

> Placed on the outer mantle of the moderator covering a Pb target and irradiated with 10 mA/1.5 GeV protons for one month, 0.3% of ^{129}I could be transmuted into ^{130}Xe, and 6% of ^{237}Np could be transmuted into ^{238}Np.

Again all technological aspects of this transmutation process had to be neglected. The emphasis of this work was on providing concrete estimates for transmutation rates under well-defined experimental conditions using GeV protons and extended targets. Furthermore, one can give a rough estimate—just as an internal consistency check—of the effective transmutation cross-section $\sigma(n,\gamma)$ for ^{129}I and ^{237}Np using Eq. (6) and values for the calculated low-energy neutron-fluence given in Table 7:

$$\sigma(^{129}I(n,\gamma)^{130}I) = (8 \pm 4)\ b$$

$$\sigma(^{237}Np(n,\gamma)^{238}Np) = (130 \pm 60)\ b.$$

The uncertainties are very large in this indirect experimental determination due to the limitations of our experimental technique. The known $\sigma(n,\gamma)$ cross-section for ^{129}I(n,γ) ^{130}I is 30 b [22], which is considerably larger than our measurement; the $\sigma(^{237}$Np(n,γ) ^{238}Np) is 180 b, as given in Ref. [22], well within the uncertainty of our results.

3. Conclusions

1. The transmutation rates for ^{129}I and ^{237}Np have been measured under specific geometrical conditions. The absolute values of these transmutation rates are such that a 1 GeV proton accelerator with 10 mA beam-current could efficiently transmute ^{237}Np into shorter-lived ^{238}Np during 1 yr while an effective transmutation of ^{129}I would take many years under the same conditions.
2. The neutron fluxes on the surface of the paraffin moderator can be estimated experimentally and theoretically using computer codes (LAHET from Los Alamos, and DCM/CEM from Dubna). The experimentally determined thermal neutron fluxes are larger than the calculated ones. The precise reasons for this discrepancy are unknown, but one could speculate that it is correlated with an enhanced

nuclear cross-section as observed in related experiments [4,6,9,19,21] (See also the additional references in Appendix B).
3. Experiments with solid state nuclear track detectors (SSNTDs) give valuable supplementary information about the nuclear interactions within the target system used.

Acknowledgements

The authors want to thank the operating crew at the Synchrophasotron of the LHE, JINR (Dubna) for the irradiations and Director Prof. A.I. Malakov and Academician A.M. Baldin for their help. They thank also Profs. A.N. Sissakian, A.D. Kovalenko and I.A. Shelaev for their continued support of this work. The Marburg team is grateful for the generous acceptance of their research aims at the LHE. The authors thank Prof. Yu.A. Panebrashev, Drs. Shimansky and Yu.S.Averichev for their support in carrying out the irradiations of the target at the F3 focus of the DISK installation. They are also grateful to Profs. N.A. Russakovitch, V.B. Brudanin, E.A. Krasavin and Dr. V.E. Aleinikov for their support in carrying out this work.

Appendix A. Supplementary experiments on secondary neutron fluences using solid state nuclear track detectors

The radiochemical work was supplemented by some additional solid state nuclear track detectors (SSNTD) studies that provided further experimental details.

A.1. Determination of thermal and energetic neutrons on top of the paraffin moderator

An experiment was carried out with CR-39 SSNTDs, covered with ^{6}LiF as described by Zamani et al. [23]. This allowed a direct determination of the fluence of thermal neutrons and energetic neutrons at all three proton energies employed. The energetic neutrons were determined with Cd-shielding through the measurement of recoil protons within the neutron energy range of $300\,\mathrm{KeV} < E(\mathrm{n}) < 3\,\mathrm{MeV}$. Three targets were placed on top of the moderator: one close to the beam entrance, one at the centre and one at the end of the moderator. The targets were exposed to a few beam pulses of the Synchrophasotron with a total flux of approximately 10^{11} protons. In this case the proton beam flux was taken as given by the machine operators, they could not be checked independently with radiochemical sensors. The results for each experiment are given in Table 8 as the average of the three samples exposed. Compared with the results in Table 7, one finds fewer neutrons at 1.5 and at 3.7 GeV and the same number of neutrons at 7.4 GeV as compared with radiochemical sensors. Part of this discrepancy might be explained because one could not check independently the proton fluences and the beam profile in this experiment.

Table 8
Neutron fluxes (per incident proton) as observed with CR-39 SSNTD (covered with ^{6}LiF) on the outer mantle of the paraffin moderator. The energetic neutron flux $n_{energetic}$ with 300 KeV $< E(\mathrm{n}) < 3$ MeV was determined using Cd shielding

Exposure	$n_{thermal}$	$n_{energetic}$
1.5 GeV p + Pb	6 ± 2	4 ± 1
1.5 GeV p + U (Pb)	14 ± 3	9 ± 3
3.7 GeV p + Pb	18 ± 4	15 ± 4
7.4 GeV p + Pb	72 ± 18	57 ± 15
7.4 GeV p + U (Pb)	138 ± 35	36 ± 7

A.2. Estimation of neutron fluxes within the paraffin-moderator using ^{235}U and ^{232}Th as target on Lexan [24]

In this study the major emphasis was placed on the determination of relative neutron fluences inside the paraffin moderator. The experimental set-up is shown in Fig. 12. The SSNTDs were thin ^{235}U and ^{232}Th targets in contact with Lexan track detectors, the first target being sensitive to thermal neutrons, the second to fast neutrons with $E > 2$ MeV. Two "containers" were placed, one

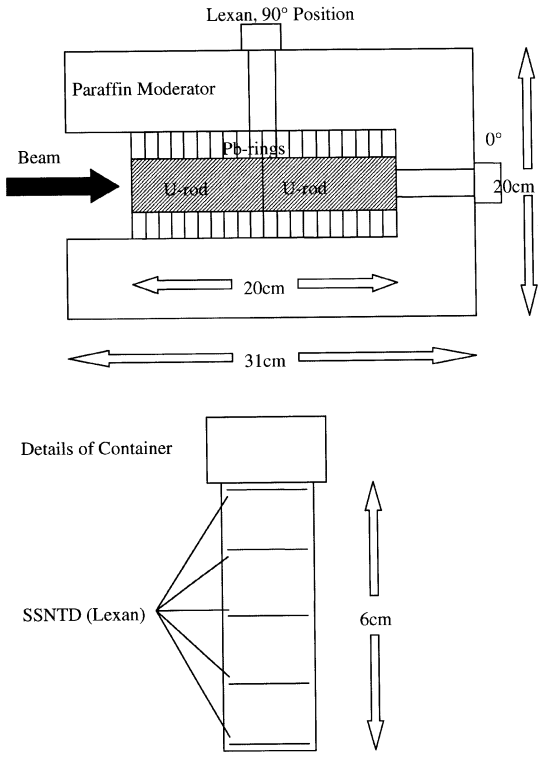

Fig. 12. Lexan SSNTDs, placed in a "container" positioned inside our experimental target set-up.

at 90° and one at 0° with respect to the beam direction. Each plastic "container" had SSNTD sensors at 4, 5.5, 7, 8.5 and 10 cm distance from the beam centre. The results are shown in Table 9. As the irradiations were carried out only with a few bursts, yielding in total approximately 10^{11} protons, the uncertainties in the absolute neutron number are large, as mentioned earlier. However, the relative yields within one "container" are quite representative.

The results (Table 9) confirm older results, as given in Ref. [9], in some more detail:

1. The effective flux of thermal neutrons is in the centre of the paraffin moderator ($d = 7$ cm) about a factor of 4 larger than in the outer mantle of the moderator ($d = 10$ cm).
2. This pattern of fluxes is the same at all primary proton energies and independent of the metallic target (U or Pb).
3. One observes in the 0°-container about the same pattern for thermal neutrons as at 90°. However, the flux of energetic neutrons ($E > 2$ MeV) increases considerably. This is to be expected from high-energy reactions.

Table 9
Effective neutrons/proton as observed inside the paraffin moderator (Fig. 13). Details will be presented elsewhere [24]

Reaction	Distance d (cm) at 90°					Distance d (cm) at 0°				
	4	5.5	7	8.5	10	4	5.5	7	8.5	10
1.5 GeV p + U										
^{235}U[a]	23	34	32	25	7	19	26	25	16	7
^{232}Th[b]	13	—	8	—	6	50	—	—		72
7.4 GeV p + U										
^{235}U[a]	130	218	277	167	59	—	—	—	—	—
^{232}Th[b]	36	—	191	—	22	—	—	—	—	—
7.4 GeV p + Pb										
^{235}U	—	27	32	17	8	18	22	23	13	5
^{232}Th	—	—	7	—	17	37	—	42	—	48

[a] Results for thermal neutrons, as measured with ^{235}U.

[b] Results for high-energy neutrons ($E > 2$ MeV), as measured with ^{232}Th. (The uncertainties are about 20%, not taking into account the uncertainties in the measurements of the proton fluxes.)

A.3. The distribution of thermal and epithermal neutrons on top of the paraffin moderator in the (7.4 GeV p + Pb) experiment [25]

Two strips of LR-115- II B SSNTDs of length 31 cm and width of $\sim$1 cm were placed on top of the paraffin moderator during the 7.4 GeV p + Pb irradiation. One of the strip was covered with a Cd foil. The detector without Cd covers registered the thermal and epithermal neutrons through ^{10}B(n,α)-^{7}Li-reactions while the detector with Cd cover registered mainly the epithermal neutrons. The results (Fig. 13) confirm that the flux of the thermal neutrons even at this large proton energy of 7.4 GeV is well centred about 11 cm behind the entrance of the beam into the lead. Furthermore, a more detailed picture on how neutrons are distributed on the moderator surface, is obtained, in particular a hump in the middle of the distribution and just above the lead target cylinder. At present it is not clear whether such behaviour has any dependence on proton energy and target type or not. The distribution of the epithermal neutrons is also shown in Fig. 13 (Ref. [25]).

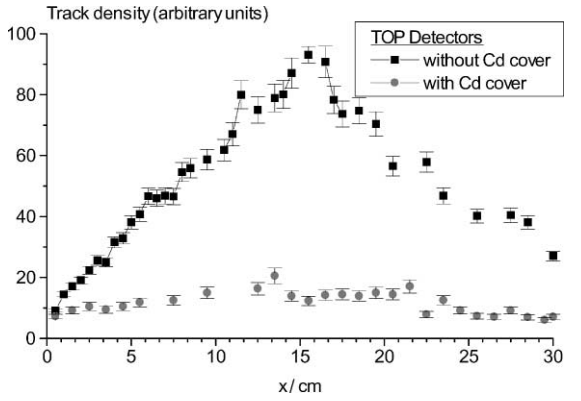

Fig. 13. Thermal (without Cd cover) and epithermal (with Cd) neutrons detected on top of the moderator with LR-115-II B SSNTDs [25], as observed in the reaction 7.4 GeV p + Pb.

A.4. The hardness of neutron spectra along the top of the paraffin moderator at 1.5 and 7.4 GeV irradiations [26]

Another technique to determine the hardness of the neutron-spectra at a certain geometrical position with the help of SSNTD has been employed. The details of the experiment will be published separately [26]. Essentially, fission cross-sections are determined with a variety of actinoide nuclides having a different threshold for (n,f)-reactions. Here, we show the results for the ratio $S = \sigma_f(^{238}U)/\sigma_f(^{235}U)$ for all four irradiations described earlier. Thin actinoides are placed on the SSNTD and irradiated on top of the moderator. The samples were etched to reveal fission tracks. The track density on the surface of the SSNTD was determined using optical microscopes. The results (Figs. 14 and 15) show that the ratio S is rather small close to the entrance of the beam into the metallic target ($d = 7$ cm), remains fairly constant over the main part of the moderator, and increases sharply close to the downstream end of the moderator, indicating a drastic increase of high-energy neutrons (> 2 MeV) inducing fission in ^{238}U. As we have placed the ^{129}I target close to the beam entrance and ^{237}Np targets more downstream, both target systems are exposed to *different* neutron spectra: ^{237}Np is exposed to a much harder spectrum than ^{129}I. However, as has been explained earlier, the uncertainties in the determination of (n,γ)-cross-sections are at present too large to allow further considerations.

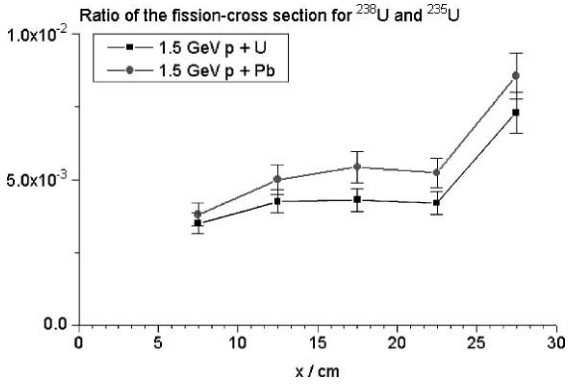

Fig. 14. Ratio S of the cross-section for the fission of ^{238}U and ^{235}U on top of the moderator during the Pb- and U(Pb)-targets [26] experiments with 1.5 GeV protons.

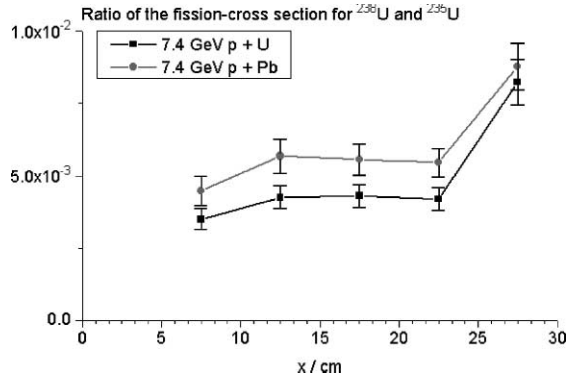

Fig. 15. Ratio S of the cross-section for the fission of ^{238}U and ^{235}U—on top of the moderator during the Pb- and U(Pb) target [26] experiments with 7.4 GeV protons.

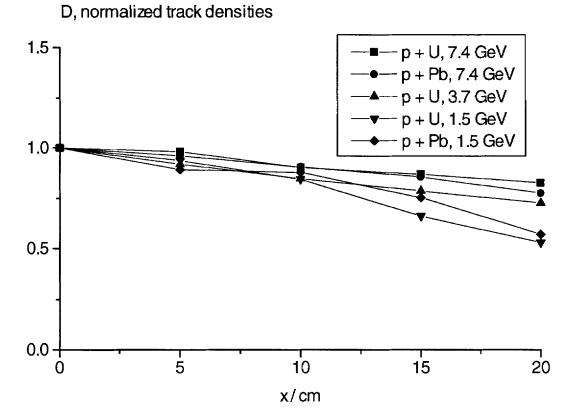

Fig. 16. Normalized track densities in CR-39 detectors attached to the metallic surfaces of the 20 cm long Pb or U(Pb) targets [27].

A.5. The part ($E > 10$ MeV) of the neutron flux on the surface of the metallic target

Thin slides of CR-39 (20 cm long, 1 cm wide and 1 mm thick) were placed along the axis of the metallic targets at the three energies investigated.

This SSNTD is—after proper etching—sensitive to energetic hadrons of energies in the range of 10 MeV. The density of recoil protons is counted and their decrease along the axis is shown in Fig. 16. The track density decreases less steeply the larger the incoming primary proton energy is. This effect has been observed in related experiments earlier [19]. See Ref. [27] for further discussions on these results.

A.6. The part ($E > 30$ MeV) of the neutron flux on the surface of the metallic target

Finally, secondary neutrons with $E > 30$ MeV were studied. Such energetic particles can induce fission in gold. Thin layers of gold with target thickness T from 0.93 to 1.65 mg/cm^2 were evaporated on the surface of 1 cm^2 annealed mica plate and placed in the centre of the 20 cm long metallic target between the metal and the paraffin moderator. After the exposure the mica was etched and a track density D was determined by optical observations (Table 10). Details will be published elsewhere [28].

When one takes an average experimental fission cross-section in gold for protons with energies 0.0 $3 < E_P < 7$ GeV of approximately 100 mb [29] and when one assumes that high-energy protons and

Table 10
Track density D, target thickness T and a normalized track density $D/\Phi T$. The total uncertainty is approximately 20%

Experiment	D (Tracks/cm^2)[a]	T/(mg Au/cm^2)[b]	$D/\Phi T$[c]
1.5 GeV p + Pb	5070	1.59	2.2×10^{-10}
1.5 GeV p + U(Pb)	5340	1.46	2.4×10^{-10}
3.7 GeV p + Pb	20 900	0.93	18×10^{-10}
3.7 GeV p + U(Pb)	33 700	0.98	28×10^{-10}
7.4 GeV p + Pb	22 300	1.54	16×10^{-10}
7.4 GeV p + U(Pb)	19 100	1.65	12×10^{-10}

[a] Track density; uncertainty: 2%.
[b] Target thickness; uncertainty: 5%.
[c] Normalized track density; the fluence Φ is taken from Table 7.

neutrons have about the same fission cross-section, then one can estimate a high-energy fluence ($E > 30$ MeV) of approximately 0.7 neutrons per 1.5 GeV p, 3.0 neutrons per 3.7 GeV and 7.4 GeV p interacting with the Pb target. This is in approximate agreement with theoretical estimations: DCM-CEM gave at (1.5 GeV p + Pb) about 1.6 neutrons, LAHET gave at (3.7 GeV p + Pb) about 2.5 neutrons.

A.7. Beam profile measurements within the thick metal targets

The beam profile has been measured by using a LAVSAN-SSNTD in contact with the 8 cm diameter Pb in contact with the front of the metal targets. The second detector was placed 10 cm, the third 20 cm downstream. This system was exposed to the entire proton irradiation. Afterwards, the LAVSAN foil was etched and the fission track density distribution along the 8 cm diameter was measured using an optical microscope. An example is shown in Fig. 17 for the 1.5 GeV proton irradiation. At 7.4 GeV proton energy the beam is better focused by a factor of 2. Another interesting feature of these measurements is the variation of track densities as a function of depth within the metal target. For 7.4 GeV protons, one observes an increase in track densities within the first 10 cm of the targets, and then a decrease. At 3.7 GeV one observes a decrease of $(50 \pm 15)\%$ between the first and the last detector, at 1.5 GeV an even stronger decrease as shown in Fig. 17. Details will be published elsewhere [30]. A similar behaviour of relativistic protons in thick targets has been determined in an independent experiment [19].

Fig. 17. The beam profile of the Synchrophasotron for an extracted 1.5 GeV proton beam: in front of the target ($z = 0$ cm), in the middle of the target ($z = 10$ cm) and at the end of the target (20 cm) in a U(Pb) target, as measured with Lavsan SSNTD in contact with Pb. The track denstiy (T/cm

Appendix B. Additional References

The contents of this article were published as preprint JINR E1-99-1 (1999) by the Joint Institute for Nuclear Research, Dubna, Russia. Due to some delays in the completion of this special issue for NIM-A, the collaboration has published (or submitted for publication) in the meantime further papers on this work, either as collective papers or as sub-group contributions.

- Refs. A2, A4, A6, A7, A10, and A12 also contain further general comments on conceptional and social aspects of transmutation technology.
- Ref. A1, A3, A5, A8, A9, and A11 contain further experimental results.

(A1) Brandt, R., M. Ochs, J.-S. Wan, Th. Schmidt, E.-J. Langrock, P.Vater, J.Adam, V.P. Bamblevsky, V.Bradnova, L.K. Geloviani, V.K. Kalinnikov, M.I.Krivopustov, B.A.Kulakov, A.N. Sosnin, V.P. Perelygin, V.S. Pronskikh, V.I. Stegialov, V.M. Tsoupko-Sitnikov, G.Modolo, R.Odoj, P.-W. Phlippen, A.-C. Adloff, F. Pape, M. Debeauvais, M. Zamani, S.R. Hashemi-Nezhad, K.K. Dwivedi, S.L. Guo, L. Li, Y.-L. Wang, and B. Wilson, (Marburg–Dubna–Juelich–Strasbourg–Thessaloniki–Sydney–Shillong–Beijing–Los Alamos) Transmutation studies using SSNTD and radiochemistry and the associated production of secondary neutrons. Radiation Measurements, 31 (1999) 497–506.

(A2) Kulakov, B.A., J. Karachuk, L.K. Geloviani, T.G. Gridnev, A.N. Sosnin, R. Brandt, (Dubna–Marburg) On the different experimental behavior of fast particles produced in 12-C interactions at relativistic energies. JINR-Dubna